PUB-75-126-E
E-0098

Inclusive Hadron Production in ~~Elastic~~ Inelastic Muon-Proton Scattering at 150 GeV/c*

W.A. Loomis, H.S. Matis, H.L. Anderson, V.K. Bharadwaj, N.E. Booth, R.M. Fine, W.R. Francis, B.A. Gordon, R.H. Heisterberg, R.G. Hicks, T.B.W. Kirk, G.I. Kirkbride, L.W. Mo, L.C. Myrianthopoulos, F.M. Pipkin, S.H. Pordes, T.W. Quirk, W.D. Shambroom, A. Skuja, L.J. Verhey, W.S.C. Williams, Richard Wilson, S.C. Wright.

Enrico Fermi Institute, Chicago, Illinois 60637
Department of Physics, Harvard University, Cambridge, Mass. 02138
Department of Physics, University of Illinois at Urbana-Champaign, Urbana, Illinois 61801
Oxford University, Nuclear Physics Laboratory, Keble Road, Oxford, OX1 3RH, England

Inclusive hadron production in muon-proton inelastic scattering has been measured for $q^2 > 0.5$ $(GeV/c)^2$ and $10 < \nu < 135$ GeV. The results are presented in the form of the transverse momentum distribution of charged hadrons and the hadron invariant structure function $F(x')$. Results are given for different regions of q^2 and s.

*Supported by ERDA Contracts No. AT(11-1)-3064 and -1195, NSF Contract No. MPS 71-03-186, and the Science Research Council (UK).

We report here on part of a comprehensive muon-proton scattering experiment at the Fermi National Accelerator Laboratory. This paper discusses the results of measurements of the inclusive charged-hadron cross sections for the process $\mu + p \rightarrow \mu^+ + h^\pm + x$.

Muon-proton scattering is dominated by the exchange of a single virtual photon and the kinematics can be characterized by q^2, the magnitude of the four-momentum squared, and by ν, the energy transferred by the photon. The differential muon scattering cross section $d^2\sigma_\mu/dq^2d\nu$ can be expressed in terms of a virtual photon flux $\Gamma(q^2, \nu)$ and the virtual photon total cross section: $d^2\sigma_\mu/dq^2d\nu = \Gamma(q^2, \nu)\sigma(q^2, \nu)$. In the center of mass of the virtual photon and proton, the kinematics of a produced hadron will be described by its momentum transverse to the photon direction p_T, by the total c.m. energy $s = M_p^2 + 2M_p\nu - q^2$, and by the value of a Feynman scaling variable $x' = p_{\|}^*/(p_{max}^{*2} - p_T^2)^{1/2}$, where $p_{\|}^*$ is the hadron's longitudinal center-of-mass momentum and p_{max}^* is the maximum value this momentum can have. In calculating x', we assume every hadron is a charged pion since no identification of hadrons is made.

The number of hadrons per virtual photon in a particular phase-space region is given by the invariant expression:

$$\frac{1}{\sigma(q^2,s)} E \frac{d^3\sigma(q^2,s)}{dp^3} = \frac{1}{\sigma(q^2,s)} \frac{1}{\pi} \frac{E^*}{(p_{max}^{*2} - p_T^2)^{1/2}} \frac{d^2\sigma(q^2,s)}{dp_T^2 dx'} \quad (1)$$

E and p are the laboratory values of the hadron's energy and momentum, E^* is the hadron energy in the center of mass.

The invariant structure function is defined by:

$$F(x', q^2, s) = \frac{1}{\sigma(q^2, s)} \frac{1}{\pi} \int_0^{\infty} dp_T^2 \frac{E^*}{(p_{max}^{*2} - p_T^2)^{1/2}} \frac{d^2\sigma(q^2, s)}{dp_T^2 dx'} \quad (2)$$

The transverse momentum distributions are given as values of:

$$G(p_T^2, q^2, s) = \frac{1}{\sigma(q^2, s)} \frac{1}{\pi} \int_{x_1'}^{x_2'} dx' \frac{d^2\sigma(q^2, s)}{dp_T^2 dx'} \quad (3)$$

Figure 1 is a schematic drawing of the experiment (a complete description will be published elsewhere). Muons of 150 GeV/c strike a 1.19-meter LH_2 target upstream of the spectrometer. The momentum of the incident muons is measured by the proportional chambers SO and magnet 1E4. Muons that scatter through sufficient angle or lose sufficient energy strike counter hodoscopes G, H, M, and trigger the apparatus in coincidence with the beam counters B. V and N counter hodoscopes veto halo muons and beam muons that do not interact. The multiwire chambers S1, S2 and S3 measure the momentum of hadrons and muons using magnetic bending in the magnet CCM (transverse-momentum kick of 2.2 GeV/c). The 2-meter iron absorber A absorbs the hadrons and the scattered muon is identified using chamber S4. The spectrometer has high muon acceptance for all q^2 and ν (except for $q^2 < 1.5$ $(GeV/c)^2$ where ν must be above 90 GeV). Hadrons are accepted by our apparatus

only in the region $x' > 0$. Events are selected for analysis as follows:

Triggers with suitably reconstructed incident and scattered-muon tracks provide $\sigma(q^2, s)$ and candidates for hadron reconstruction. All hadrons are accepted with reconstructed tracks in spark chamber modules S2, S3 which link through the CCM to tracks in S1. In addition, appropriate hodoscope counters along the tracks must be struck and the tracks must pass through the muon-scattering vertex. The vertex resolution enables us to exclude from consideration all material except the liquid hydrogen, the target flask end windows, and the downstream end of the aluminum vacuum vessel. The liquid hydrogen constitutes 95.4% of the target mass as defined (verified by empty-target runs).

Only the electric charge and momentum of the hadrons is measured. Electron contamination from π^o photon conversion is less than 3%. Muon-electron scattering events are eliminated by a kinematic cut demanding $q^2 \geq 0.5\ (GeV/c)^2$. Corrections are made to the hadron spectra for acceptance, track reconstruction and re-interaction in the target as follows:

Each observed hadron is weighted by an acceptance in x' and p_T^2. This acceptance is determined by the direction of the virtual photon for the particular event. The virtual photon directions vary with respect to the apparatus. This leads to regions of zero acceptance in $x' - p_T^2$ with boundaries which are

q^2 - s dependent. Only muon scatters that can contribute to a particular x' - p_T^2 bin are used in the evaluation of F(x') or $G(p_T^2)$.

Six percent of the muon-produced hadrons undergo secondary interactions in the target. The x' of secondary hadrons is always reduced from that of the primary hadrons. The induced migration of data is such that any data point is affected only by data points of smaller cross section. We correct only for the 6% loss. The overall reconstruction efficiency of the hadrons is estimated to be 90 ± 5%. The precision in the measurement of x' and p_T^2 has negligible effect on the hadron distributions.

F(x') is formed by taking the total number of hadrons near x' having q^2 - s within the region specified. This is divided by the total number of muons in the q^2 - s region along with appropriate kinematic factors. Weighting the muons and corresponding hadrons by the muon acceptance has no effect on the results. Radiative corrections are not made to the number of hadrons or to their apparent x' and p_T^2. The number of muons is reduced by the calculated number of radiative elastic muon scatters, this calculation using the formulae of Mo and Tsai[1].

The results are presented in Figs. 2-5. Figure 2 shows $G(p_T^2)$. For all q^2, s and x' regions studied, the best fits were found to be of the form:

$$G(p_T^2, q^2, s) = G(p_T^2) = A \exp\left[-b(p_T^2 + M^2)^{1/2}\right] \quad (4)$$

The results of these fits are shown in Fig. 3 as functions of s and x'. No discernible q^2 variation was seen. In Fig. 3, b, typical of high p_T^2 behavior, shows no variation with s or x'. M, typical of low p_T^2 behavior, seems to increase with x'. Equivalently the low p_T^2 slope of the data decreases with x'.

F(x') is shown in Fig. 4 broken into q^2 - s regions. The dotted line is .35 exp (-3.25x') allowing a comparison of the data in the different regions. This line is also a good representation of F(x') for negative hadrons as measured by Dakin et al.[2] at lower energies. This measurement shows no statistically significant variation of F(x') with q^2 and s. Fig. 5 shows the charge ratio N^+/N^- as a function of q^2, s and x'. For x' < 0.4 the ratio is 1, within statistics, as it must be for high energy events. For x' > 0.4 the data suggest a small positive charge asymmetry whose dependence on q^2 and s is unclear.

We conclude the following:

(1) The hadron spectra show no substantial q^2 - s variation. (2) The spectra are in agreement with previous measurements[3] of virtual photon-hadron production. As must be expected, the earlier charge asymmetry has largely vanished at higher energies. (3) While there are differences, the data are typical of hadron-hadron interactions.[4]

We thank Fermilab for the use of their facilities and their energetic assistance. We are grateful for the technical assistance

provided by the staffs at our home institutions and at the Rutherford Laboratory without whose expert help the experiment could not have been mounted.

References

1. L.W. Mo and Y. Tsai, Revs. Mod. Phys. 41, 247 (1969).

2. J.T. Dakin et al., Phys. Rev. 10D, 1401 (1974).

3. C.J. Bebek et al., Phys. Rev. Lett. 30, 624 (1973); 32, 27 (1974); 34, 759 (1975); 34, 1115 (1975); also, see Ref. 2, above.

4. J. Whitmore, Phys. Lett. 10C, 273 (1974); R. Slansky, Phys. Lett. 11C, 101 (1974).

Figure 1. Plan view of spectrometer. SO, S1 are multiwire proportional chambers; S2, 3, 4, 5, 6 are multiwire spark chambers; B, G, H, M, N, V are counter hodoscopes; 1E4, CCM are magnets; R, C, A are absorbers.

Figure 2. Typical transverse momentum spectrum for charged hadrons. Two x' ranges are shown, the fits are of the form $A \exp\left[-b(p_T^2 + M^2)^{1/2}\right]$ and apply to the negative hadrons as shown in Fig. 3.

Figure 3. Two-parameter fit to transverse momentum distribution of inclusive hadrons (Eq. 4). Lo x' means $0.2 < x' < 0.5$; Hi x' means $0.5 < x' < 1.0$; Lo s means $20 < s < 100$; Hi s means $100 < s$.

Figure 4. Invariant longitudinal momentum spectrum for charged inclusive hadrons in several intervals of q^2 and s. The dotted line is $.35 \exp(-3.25x)$.

Figure 5. Ratio of positive to negative charged hadrons as a function of q^2 for selected s, x' intervals.

S0
S0
IE4
S0
S0
B
9M
V
3M
LH
S1
CCM
MAGNET
S1
S2
S2
S2
H
S3
G
R
C
S5
S6
A
NM
S4

FIG 1

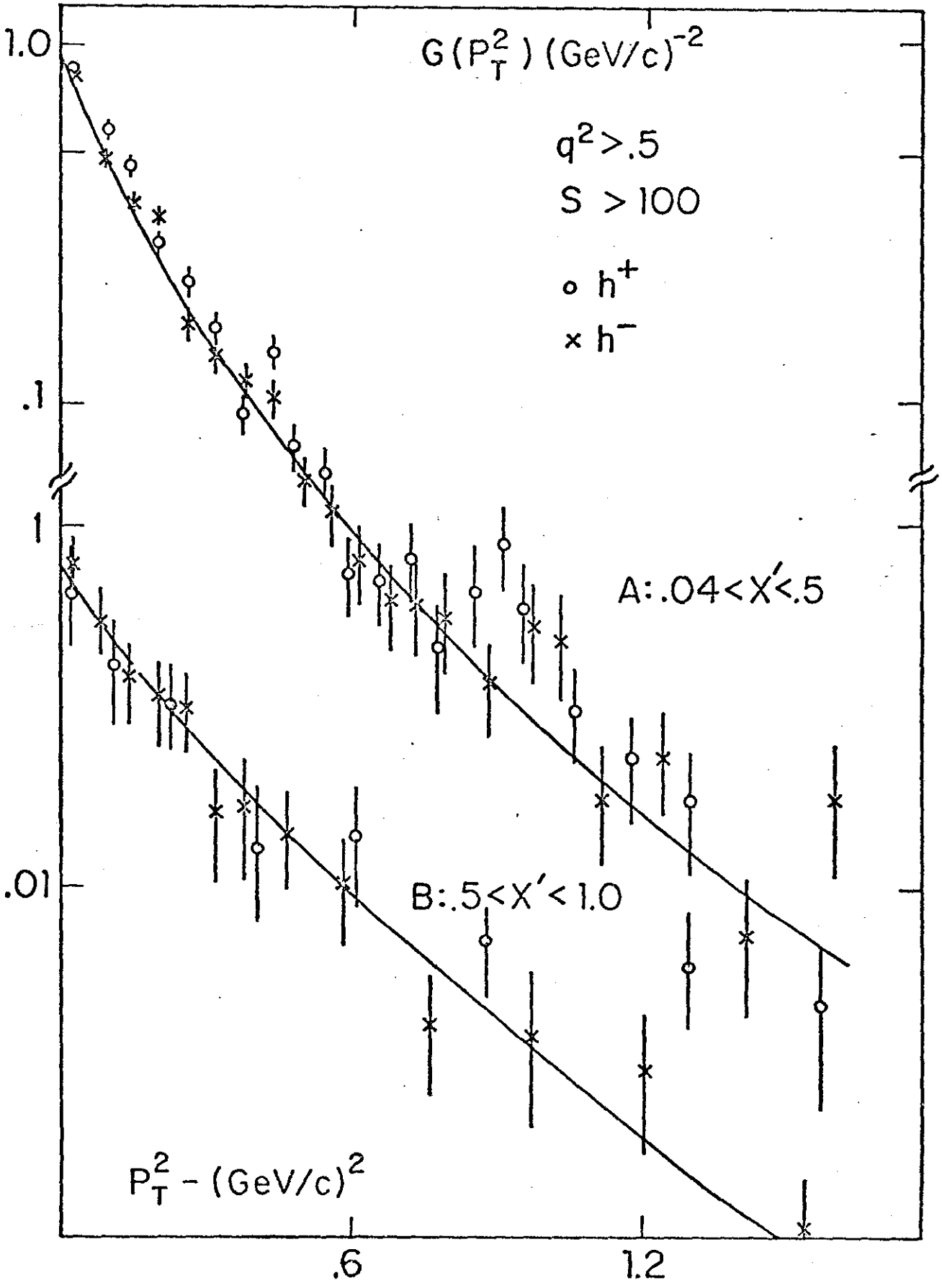
1.0
.1
1
.01
$G(P_T^2)$ $(GeV/c)^{-2}$
$q^2>.5$
$S>100$
$\circ$ h^+
$\times$ h^-
A: $.04<X'<.5$
B: $.5<X'<1.0$
P_T^2 - $(GeV/c)^2$
.6
1.2

FIG 2

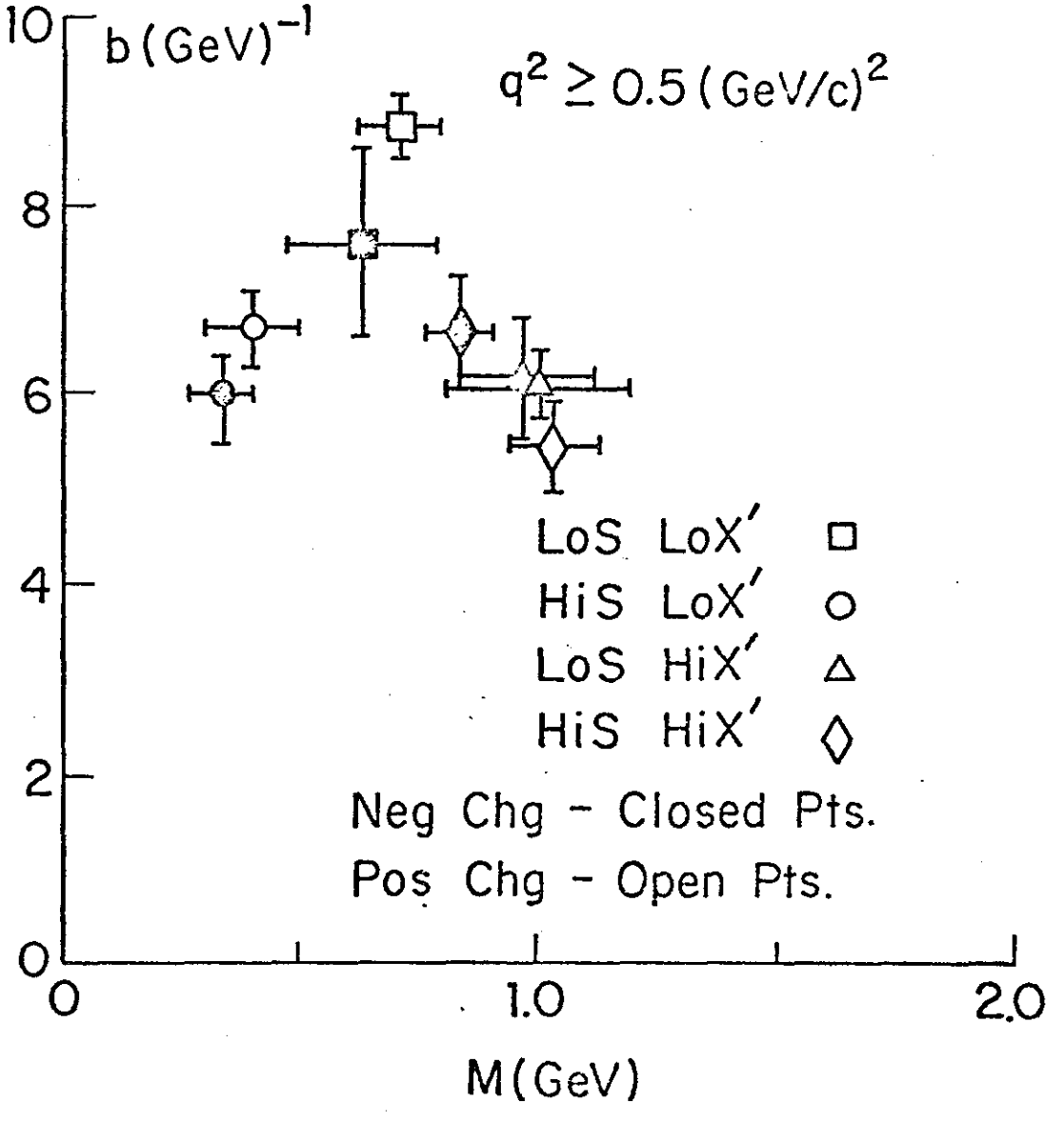
10
b (GeV)$^{-1}$
$q^2 \geq 0.5$ (GeV/c)^2
8
6
4
2
0
0
1.0
2.0
M(GeV)
LoS LoX′
HiS LoX′
LoS HiX′
HiS HiX′
Neg Chg - Closed Pts.
Pos Chg - Open Pts.

Fig 3.

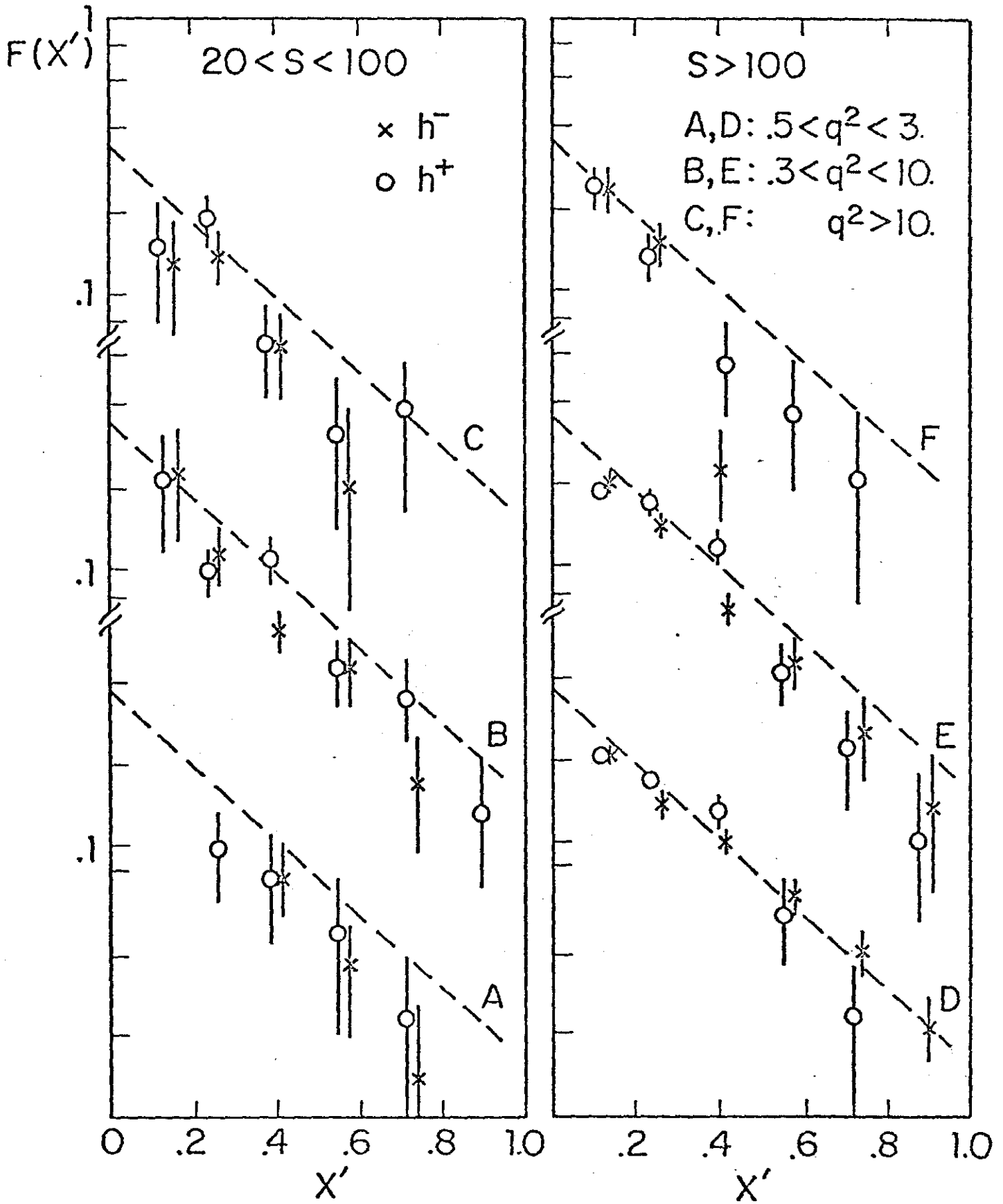
F(X')
1
.1
.1
.1
20<S<100
× h⁻
o h⁺
S>100
A,D: .5<q²<3.
B,E: .3<q²<10.
C,F: q²>10.
A
B
C
D
E
F
0
.2
.4
.6
.8
1.0
X'
.2
.4
.6
.8
1.0
X'

FIG 4

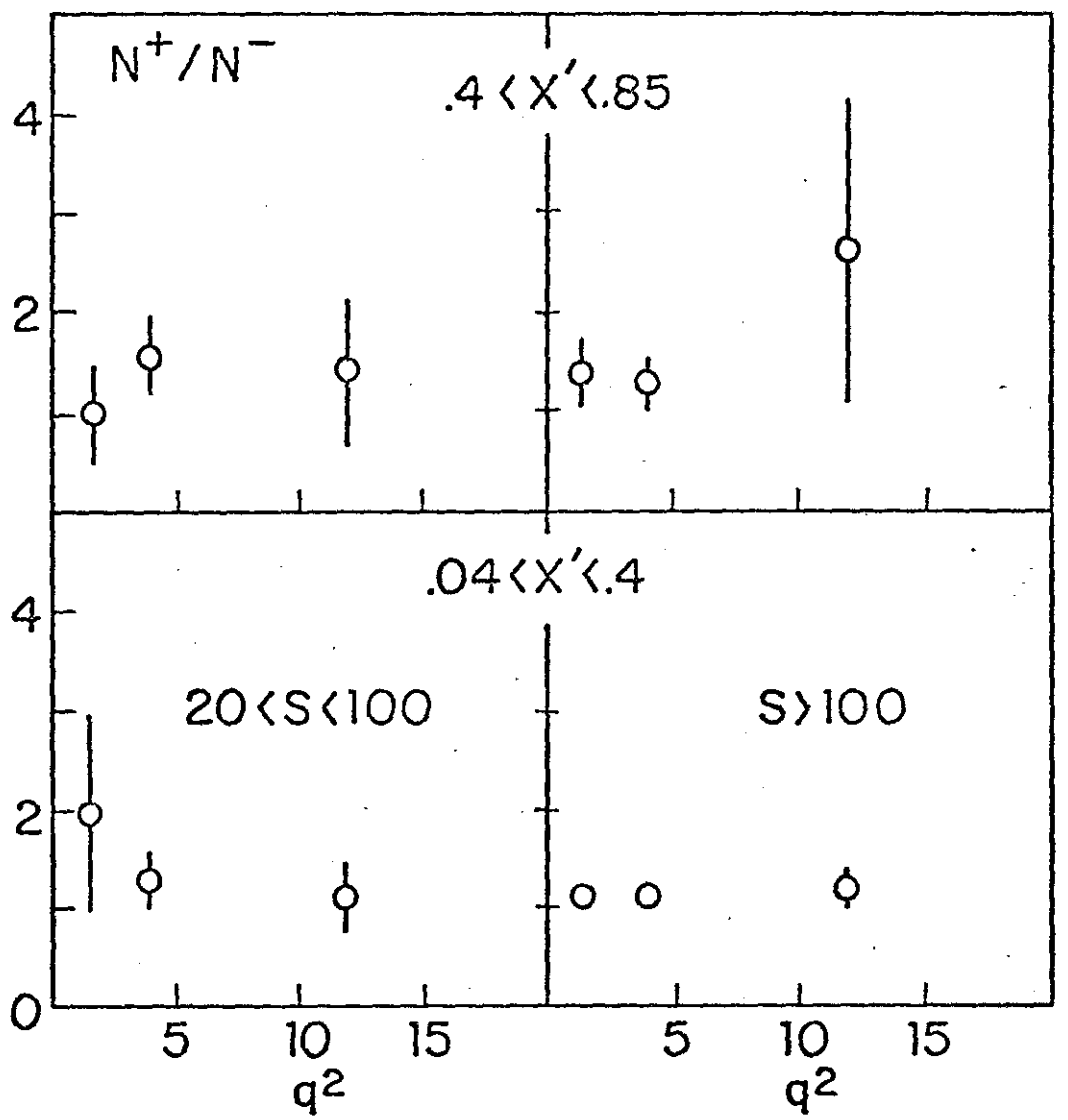

FIG 5